

OPERATIONAL FORECAST OF OILSPILL TRAJECTORY AND ASSESSMENT OF IMPACTS ON INTERTIDAL MACROBENTHOS IN THE DAHANU REGION, WEST COAST OF INDIA

Velamala Simhadri Naidu¹, Soniya Sukumran¹, Om Dubbwar¹, G. Sidda Reddy²

1. National Institute of Oceanography, Regional Centre, Lokhandwala Road, 4 Bungalows, Andheri (W), Mumbai – 400 053, India Email: vsnaidu@nio.org (Corresponding Author).
2. Environ Software Pvt Limited, Environ Towers, Hosur Road, Konappana Agrahara, Electronic city, Bangalore – 560100, India

ABSTRACT

A 2D model has been developed and applied to the hypothetical spills of crude oil in the Dahanu area, west coast of India. An attempt has also been made to quantify the intertidal macrobenthic biomass and population affected in the region. Data on tides and currents were collected at Dahanu during October and November 2008. The currents recorded at relatively offshore location show that the mid currents were stronger than the bottom currents. The currents at nearshore location were influenced by the Dahanu creek currents. Offshore currents were relatively stronger than the nearshore currents. The model calibration results of hydrodynamics show that the circulation was almost in agreement with the observations except in the creek zone.

Oil spill model was run for two different weather conditions, viz, postmonsoon and monsoon. An instantaneous crude oil spill of 500 t (534 m³) was considered. The results show that the spill would move offshore in the presence of postmonsoonal winds. However, during the monsoon the spill would move towards the coast. According to the positions of the occurrence, the spill would reach the coast within 13 to 28 h from the time of spill. The coastline stretches affected range from 2.1 km to 2.8 km. The estimated affected macrobenthic biomass and population would be 109.2 – 145.6 kg and 1.9 – 2.5 x10⁷ respectively. The major species affected would be polychaetes.

Key words: Oil spill, Model, Tides, Currents, Intertidal, Benthos, Lagrangian circulation, Dahanu.

Introduction

A potential oil spill is the most significant risk to manage in the event of accidental spills occurred during transportation. Nearly half of the world production of oil has been transported by the sea route (Clark 1992). From 1988 to 1991, 28 oil spills of 500,000 L (132,100 gal) or more occurred (Yapa 1996). The total volume of oil spilled from major spill, excluding Arabian Gulf/Kuwait spill, for the same period was 293,000,000 L (77,400,00 gal). The 1991 Arabian Gulf/Kuwait spill was estimated at 143 billion L or 37.8 billion gal. To contain the environmental damage caused due to the spill, measures should be taken effectively and quickly. It is essential to know the trajectory of the spill and its likely target on the shoreline. Prediction of the oil movement will help in appropriate decision making for spill response and in directing the available resources effectively.

Oil spill models are extensively used for quantitative assessments of environmental impacts resulting from accidents. An accidental spill in coastal waters can cause enormous damage to the ecosystem, recreational facilities, and poses threats to water supplies for the areas depend on desalinated sea water or rivers and lakes to supply fresh water. Hence, assessments are required for those spill scenarios for planning and management decision-making to minimise the biological and other environmental impacts. The damage to the natural resources can be reduced by developing comprehensive oil spill polices and good contingency plans. One of the most aspects is predicting, spreading and transport of oil slick. The fate and transport of the oil spill is governed by (a) advection due to current and wind, (b) horizontal spreading of the surface slick due to both turbulent diffusion and gravitational, inertia, viscous, and surface tension forces, (c) emulsification (d) mass transfer and change in physicochemical properties of oil due to weathering processes such as evaporation, entrainment (dispersion) and dissolution and (e) and interaction of oil with the shoreline.

Keeping the severity of the problem in view, Ministry of Earth Sciences (MoES), Government of India, has taken up a study related to the oil spill modeling along the India coast line. As a part of the project, this work has been carried out.

Spills occurred near Mumbai harbor, which is barely 100 km south of study area, on 07th August 2010 and 04th August 2011 showed the need for the forecast of the spilled oil. The spill movement was predicted off the Goa coast by Vethmony et al (2007). The risk assessment of accidental spillage in the Gulf of Kachchh was studied by Kankara and Subramanian (2007). Impacts of the *Pacific*

Adventures oilspill on the macrobenthos of sandy beaches were studied by Thomas et al (2011). The oil spill on the beaches even though small quantities can cause much damage and recovery may be slow (Gesteira and Dauvin 2005). However, no study on oil spill has been carried out at Dahanu region which is surrounded by several industries, viz, Reliance Power, Tarapur industrial estate and shipping routes etc (Fig. 1). Recently Oil and Natural Gas Commission (ONGC) has found oil off Dahanu region. In this work, an attempt has been made to study the hydrodynamics of the Dahanu region and to develop a suitable model to predict the spill track and to estimate the fates of the oil spill.

The spreading of oil in the open ocean has been studied extensively by several authors, Binliang Lin and Falconer 1996; Brunet and Reddy 1997; Reddy and Brunet 1997. The boundary fitted grid technique makes the equation and boundary conditions simple and better representation of the complex geometry with a relatively less number of grid points.

Materials and Methods

Modeling of Hydrodynamics

Continuity equation is:

$$\frac{\partial \eta}{\partial t} + \frac{\partial uH}{\partial x} + \frac{\partial vH}{\partial y} = 0 \quad (1)$$

where η = water elevation with respect to mean sea level, $H = (h + \eta)$ total water depth and h = water depth with respect to mean sea level.

The depth-averaged momentum equations in x and y directions are:

$$\frac{\partial uH}{\partial t} + \frac{\partial u^2H}{\partial x} + \frac{\partial uvH}{\partial y} = fvH - gH \frac{\partial \eta}{\partial x} + H \frac{\partial}{\partial x} \left(K_x \frac{\partial u}{\partial x} \right) + H \frac{\partial}{\partial y} \left(K_y \frac{\partial u}{\partial y} \right) + \frac{\tau_{wx}}{\rho} - \frac{\tau_{bx}}{\rho}, \quad (2)$$

$$\frac{\partial vH}{\partial t} + \frac{\partial vuH}{\partial x} + \frac{\partial v^2H}{\partial y} = -fuH - gH \frac{\partial \eta}{\partial y} + H \frac{\partial}{\partial x} \left(K_x \frac{\partial v}{\partial x} \right) + H \frac{\partial}{\partial y} \left(K_y \frac{\partial v}{\partial y} \right) + \frac{\tau_{wy}}{\rho} - \frac{\tau_{by}}{\rho}, \quad (3)$$

Where t = time; ρ = density of sea water; f = coriolis parameter; g = acceleration due to gravity; x, y are Cartesian co-ordinates; u and v are depth averaged velocity components; K_x, K_y diffusion coefficients; τ_{wx}, τ_{bx} and τ_{wy}, τ_{by} = wind and bottom stresses in x and y directions respectively.

The horizontal diffusion coefficients K_x and K_y are calculated as:

$$K_x = \alpha_x gH \left(\sqrt{u^2 + v^2} \right) / C^2 \quad (4)$$

$$K_y = \alpha_y gH \left(\sqrt{u^2 + v^2} \right) / C^2 \quad (5)$$

where, $\alpha_x = 0.15$ and $\alpha_y = 0.15$ are the depth averaged eddy viscosity coefficients in x and y directions. C is the Chezy's coefficient calculated using the Manning's roughness (n) coefficient as $C = 1/n R^{1/6}$, where R = hydraulic radius = A/P (A is wetted area and P is wetted perimeter) and can be equal to flow depth in case of shallow waters.

The diffusion coefficients for horizontal exchange of momentum vary in space. The wind stress in the x and y directions (τ_{wx}, τ_{wy}) can be written as:

$$\tau_{wx} = \rho_a C_d U_w \left(\sqrt{U_w^2 + V_w^2} \right) \quad (6)$$

$$\tau_{wy} = \rho_a C_d U_w \left(\sqrt{U_w^2 + V_w^2} \right) \quad (7)$$

where, $U_w, V_w =$ wind velocity components in x and y directions respectively, $\rho_a =$ air density, $C_d =$ air water drag coefficient. The bottom stress in the x and y directions (τ_{bx}, τ_{by}) can be written as:

$$\tau_{bx} = \rho g u \left(\sqrt{u^2 + v^2} \right) / C^2 \quad (8)$$

$$\tau_{by} = \rho g v \left(\sqrt{u^2 + v^2} \right) / C^2 \quad (9)$$

where, τ_{bx} and $\tau_{by} =$ bottom stress components in the x and y directions respectively.

Boundary-Fitted Coordinate (BFC) system.

In the present study, BFC system has been used to resolve complex topography in horizontal direction. The continuity equation can be written in BFC system using chain rule transformation as:

$$\frac{\partial \eta}{\partial t} + \frac{1}{J} \left(y_\xi \frac{\partial(uH)}{\partial \zeta} - y_\zeta \frac{\partial(uH)}{\partial \xi} + x_\zeta \frac{\partial(vH)}{\partial \xi} - x_\xi \frac{\partial(vH)}{\partial \zeta} \right) = 0, \quad (10)$$

Where, $x_\xi, y_\xi, x_\zeta, y_\zeta =$ grid transformation parameter, and J = Jacobian transformation. The momentum equations can also be written in BFC coordinate system in the same manner as described above (Thomson et al., 1977; Reddy, 1997; Vethamony et al., 2005).

The transformed governing equations of flow have been discretised on a staggered grid and solved using Alternating Direction Implicit (ADI) finite difference scheme. The scheme splits the time into two intervals. In the first half-time step, derivatives with respect to ζ are advanced from t^n to $t^{n+1/2}$, and the derivatives involving ξ are held at t^n . In the second half-time ζ derivatives are held at $t^{n+1/2}$ and ξ derivatives are advanced from $t^{n+1/2}$ to t^{n+1} . Non-derivative terms are computed at t^n for both levels. The transformed equations of flow are discretised using ADI procedure in ζ and ξ directions, arranged in the form of algebraic equations and grouped together to form a tri-diagonal matrix, which is then solved implicitly for tides and currents. The time step (Δt) is chosen based on the Courant stability criteria because, the BFC grid size varies both in x and y directions.

Modeling oil spill trajectory

Basic governing equation of mass transport is given as follows,

$$\frac{\partial \theta}{\partial t} + \frac{\partial u \theta}{\partial x} + \frac{\partial v \theta}{\partial y} = \frac{\partial}{\partial x} \left(D_x \frac{\partial \theta}{\partial x} \right) + \frac{\partial}{\partial y} \left(D_y \frac{\partial \theta}{\partial y} \right) \pm S_p \quad (11)$$

Where θ = Pollutant concentration of dissolved constituent (C) or temperature (T). S_p = Source or Sink term.

Typically in models using Lagrangian Discrete Parcels methods, oil is represented by a large ensemble of small parcels. The movement of each parcel is affected by the physico-chemical processes. Once the parcels are released in the water body, their discrete path and mass are followed and recorded as function of time relative to reference grid system fixed in space. Then the density distribution of ensemble can be interpreted as the concentration of the oil. Since the movement of each parcel is dependent upon the distribution of the entire ensemble, all the parcels must be traced to time level before proceeding to the next. In a Lagrangian parcels application, the total mass of the system is always conserved.

The transformed governing equations of flow have been discretized on a staggered grid and solved using Leapfrog trapezoidal scheme through predictor and corrector step method. The scheme is fully centered in space and time and can obtain 2nd order accuracy. The scheme consists of two level computations within the time step Δt , i.e. Predictor and Corrector steps.

$$F(K^n) = (K^* - K^{n-1}) / (2\Delta t) \quad \dots(12)$$

$$F(K^n) + F(K^*) = 2(K^{n+1} - K^n) / (\Delta t)$$

Where * indicates the variables at predicted time level.

The grid transformation derivatives can be specified at the cell centers and at the cell mid faces. Since the range of the coordinate in the computational plane is completely arbitrary the mesh increments are specified as unity for convenience. Consequently the geometric variables are defined on a finite difference mesh with cell increments of 0.5. The computations have been carried out for the next time step through predictor and corrector schemes using the above finite difference quotients.

Since the number of parcels on the surface and in water column continuously changes due to exchange processes, it is necessary to use an efficient data structure for storing them. The use of an array of linked lists for storing parcel information is the best known method. This results in fairly efficient storing in a packed manner, and is also ideally suited for simulations involving multiple species of contaminants. Such an algorithm has been developed and used by Yapa et al (1994). The surface or subsurface oil spill consists of slick floating on the water surface, which partially dissolves in the water and partially evaporates into the atmosphere. There is a continuous exchange between the suspended and surface oil (floating oil). The assumption made in deriving the governing equations is the thickness of the oil layer is negligible in comparison with the water depth.

In addition to the location, size, physio-chemical properties of the spill and other major factors affect the fate of the oil slick which are governed by complex interrelated transport and weathering processes. The spilled oil spreads and moves according to the forces of winds and currents. In the present model, all these processes are considered in the transport of oil.

In most of the oil spill models, drift factor approach has been used. This is considered to be the most practical method for predicting the advection of oil slicks. In this method, the mean drift velocity of the surface oil is considered to be a weighted sum of the wind velocity and depth-averaged current.

$$V = V_w \alpha_w + V_c \alpha_c \quad \text{-----}(13)$$

where, V_w = the wind velocity at 10 m above the water surface, V_c = the depth averaged velocity, α_w = the wind drift factor, α_c = current drift factor. Normally wind-induced surface currents have been

reported to vary between 1% and 6% of the wind speed, with 3% being the most widely used drift factor in oil slick models. A value of about 1.1 is generally used for α_c , assuming that the velocity distribution over the depth of flow is logarithmic.

The advective velocity of each oil parcel can be a sum of the mean and turbulent fluctuation components of the drift velocity. The turbulent fluctuation components are included in the simulation of horizontal diffusion.

The oil spilled undergoes several processes viz., advection, spreading, evaporation, dissolution, emulsification and shore deposition. In addition, photo-chemical reactions and microbial biodegradation can also change the character of the oil and reduce the amount of oil over a long duration.

Advection

Advection is a physical process which involves the drifting of the surface oil slick and the subsurface oil. It is the main mechanism governing the location of oil following its discharge. The advection of surface oil is caused by the combined effects of surface current and wind drag.

The advection velocity of each oil parcel can be computed as suggested by Shen and Yapa 1988.

$$V_t = V + V^1$$

Where V_t = drift velocity of oil parcel, V and V^1 are the mean and turbulent fluctuation components of the drift velocity respectively.

The horizontal turbulent diffusion due to turbulent fluctuations of the drift velocity is computed based on random walk analysis (Fisher et al 1979).

$$V^1 = (4D_t/\delta t)^{1/2}$$

D_t is strongly related to turbulence. In the ocean it has to be estimated based on available data or past experience. Values used for D_t vary widely. Huang and Monastero (1982) reported values ranging from 5 to 19 m^2/s . However, much wider variations can be found in the literature. In rivers, the

diffusion coefficient is affected by the shear velocity and the depth of flow h .

$$D_t = 0.6hU^*$$

δt = time step.

U^* = Shear velocity

Mechanical spreading

Fay (1969, 1971) observed that the changes in slick properties caused by weathering may result in the eventual cessation of the mechanical spreading. Based on a number of field observations, Fay suggested an empirical form to estimate the maximum area of an oil slick due to mechanical spreading as

$$A_f = 10^5 Y^{3/4}$$

In which A_f = final area in m^2 , and Y = total volume of the slick in m^3 .

The spreading of an oil slick is one of the most important processes in the early stage of the oil slick transformation. The spreading of an oil slick is determined by the balance between gravitational, viscous and surface tension forces. The spreading of an oil slick passes through the following three phases: (i) in the beginning phase, the gravity and inertia forces are balanced, (ii) in the intermediate phase, the gravity force is balanced by the viscous force and (iii) in the final phase, the surface tension force is balanced by viscous force.

Evaporation

Evaporation is the loss of oil mass to the atmosphere and occurs immediately after the spill. Spreading increases the surface slick area causing the evaporation rate to increase. The amount and rate of evaporation depend on the composition of oil, wind conditions, temperature, and surface slick area. The evaporation term is calculated basing on the equation suggested by Mackay et al (1980).

$$F = (1/C) [\ln P_o + \ln (CK_{Et} + 1/P_o)]$$

Where, F is volume fraction oil evaporated, $K_E = K_M Av / (RT V_o)$, K_E is the “evaporative exposure” term, which varies with time and environmental conditions; $K_M = 0.0025 U_{wind}^{0.78}$ is the mass transfer

coefficient in m/s; U_{wind} is the wind speed in m/s; A is spill area in square meters; R is the gas constant, $82.06 \times 10^{-6} \text{ atm m}^3 \text{ mol}^{-1} \text{ K}^{-1}$; T is surface temperature of the oil in degrees Kelvin, which is generally close to the ambient air temperature. A is the spill area and v is molar volume. V_o is the initial spill volume in m^3 , initial vapor pressure in the atmosphere (P_o) at the temperature is calculated using equation ie, $\ln P_o = 10.6[1 - (T_o/T_E)]$, $C = 1158.9 \text{ API}^{-1.1435}$, $T_o = 542.6 - 30.275 \text{ API} + 1.565 \text{ API}^2 - 34.39 \text{ API}^3 + 0.0002604 \text{ API}^4$, API is calculated using the formula ie, specific gravity = $141.5/(\text{API} - 131.5)$,

Dissolution

Dissolution is an important process to be considered for the possible biological degradation, although it only accounts for a negligible fraction of the mass balance of the oil. It is a function of oil slick area, dissolution mass transferability and oil solubility in water.

In the present study, the method of Cohen et al. (1980) is used. In this method, the total dissolution rate N (gm/h) of the slick is calculated by

$$N = KA_s S$$

where, K is the dissolution mass transfer coefficient in m/h, A_s is the slick area in m^2 , and S is the oil solubility in water. Huang and Monasero (1982) calculated the solubility for typical oil as:

$$S = S_o \exp(-0.1t)$$

where, S_o is the solubility for fresh oil and 't' is the time after the spill.

Vertical mixing and Emulsification

Emulsification is a physico-chemical processes that results in a substantial increase in the viscosity and volume of the surface layer due to the increase in water content in the slick. This increase in the water content is due to the incorporation of small water droplets into the slick as a result of the coalescence of large oil droplets back into the surface slick. The most commonly used method for computing the increase in water content and the change in the apparent viscosity of the emulsion is based on the equations developed by (Mackay et al. 1980).

$$\mu_E = \mu_o \exp [2.5W/(1-K_1W)]$$

Where μ_E and μ_o are viscosities for the emulsion and parent oil respectively. W is the water content fraction of the emulsion. K_1 is the rate constant of water incorporation.

Shoreline deposition

The shoreline deposition is calculated using the Reed formula (Reed et al 1986) in which half-life concept is adopted. The oil slick will reach the shoreline sometime after a spill occurs. Based on the half-life formulation, the volume of oil remaining on the beach can be related to its original volume by

$$V_1 = V_2 e^{-Kt}$$

where, V_1 and V_2 are volumes of the oil on the beach at times t_1 and t_2 , respectively; $K = -\ln (1/2)/\lambda$, a decay constant and λ =half-life.

Length of the shore line affected was calculated using half the slick radius method. When the oil slick reaches the coastal boundary, the radius of the slick is calculated. Now the length of the coast affected would be half of the radius of the slick.

Thickness of the oil is calculated in the model using the method that the volume of oil remained on the surface after undergoing all weathering processes is divided by the total area of the spill occupied.

Oil specifications

The crude oil with the following specification is considered for the spill.

Specific Gravity	:900 kg/m ³
Surface Tension	:3.0 e ⁻³ N/m.
Molar Volume	:0.002 m ³ /mole
Viscosity:	:7.02e ⁻⁴ (m ² /sec) at 40° C
Surface Temperature	:303 k
Ambient Air temperature	:308 k
Gas Constant	:8.206 e ⁻⁴ m ³ /mol-k
Wax content	:12 – 19 %

Results and discussion

The software has been developed based on the numerical aspects discussed earlier and run to test its efficacy in the computational flow field with the field observations made at Dahanu. The bathymetry was taken from Naval Hydrography Office (NHO) Chart 210. Under the MoES program, tide and current data were collected at 5 stations from 21.10.2008 to 10.11.2008 as shown in the Figure 1. (C denotes current, T denotes Tide measurements and TR denotes the macrobenthos transect). Aanderaa make self-recording RCM9 current meters were deployed for current direction and velocity and Valeport make tide gauges were used for recording water level observations. The data was recorded at 10 min interval. A neutrally buoyant drogue was released at Station 3 on 01.11.2008 at 0800 h. The drogue was followed by a boat equipped with Garmin make GPS. The drogue location was recorded at 30 min interval. The experiment was conducted till 1730 h.

For macrobenthic analysis, sediment collections between highest high water and lowest low water (intertidal zone) were done using quadrants (0.04 m^2) upto a depth of 10 cm in quadruplicate. The sediment was sieved through a 0.5mm mesh sieve and animals retained were preserved in 5% buffered formaldehyde-Rose Bengal solution. The macrobenthos were identified upto major taxonomic groups in the laboratory and total population is estimated (no m^{-2}). Macrobenthic biomass was determined on wet-weight basis (g m^{-2})

The tide data collected at stations 1 and 2 shows that the maximum tidal amplitudes during spring and neap at Dahanu were 5.2 m and 3.9 m respectively (Figure 2). The difference in average tidal amplitude between station 1 and 2, which are separated by 10 km distance, was 0.15 m while the time lag between these stations was 15 min. Current data were collected at station 1, 3, 4 and 5 (Figures 3, 4, 5, 6). The station 1 is located in the offshore where the depth of 25 m below Chart Datum (CD) is found. The current vectors in the location at the mid depth show that the maximum speed varied from 1.65 to 0.3 m/s in spring and neap respectively (Figure 3). Direction of the flow was between northwest and southeast ($170^\circ - 350^\circ$ with respect to north). Bottom currents reveal that the maximum speeds ranged from 0.3 to 1.2 m/s and the direction was between $180^\circ - 360^\circ$. The mid currents were relatively stronger than the bottom currents. The direction of the bottom currents remained almost same with deviation of 10° . The phases of flood and ebb are matching with mid and bottom currents. However, the bottom ebb currents (southward) were relatively variable as compared

to the flood currents. In general the currents in the region varied between north and south and vertically homogeneous conditions prevailed.

The currents recorded at stations 3 and 5, where 10 m water depth is available, show that the maximum current speeds at station 3 (0.8 m/s) were lower than those at station 5 where speed of 1.2 m/s was observed (Figures 4 and 5). Direction of the currents also varied from station 3 to 5. At station 3, the direction was between northeast and southwest while at station 5 it was more inclined (nearly 10°) towards east (Figures 4 and 5). In other words, the current was more stronger and parallel to the coast at station 5. Station 3 is situated nearer to the mouth of the Dahanu creek. Under its influence, the direction of the flow was changed in this region as compared to the station 5. The currents in the Dahanu creek (Figure 6) indicated that the maximum spring and neap values ranged from 0.9 to 0.2 m/s respectively. The direction of the flow was along the creek axis. The axes of currents in the offshore was north-south whereas it was in the north east and south west in the near shore waters.

From the above results it is found that the offshore currents were stronger than the nearshore currents and the vertical variation in the currents in the offshore location is small. The currents at mouth of the creek were influenced by the creek currents. The axis of the currents in the offshore was north-south whereas it was in northeast and southwest in the nearshore waters.

Model setup and Boundary Specifications

In the initial phase of this investigation, a model domain with 100 x 110 grids in x and y directions was used respectively. The bathymetry depth contours used in the model are shown in the Figure 7. The contours run parallel to the coast and maximum depth in the model domain is 30 m.

Tides have been prescribed at north and south open boundaries. The no-flow boundary condition has been assumed in the western side. The initial conditions for model has been selected based on Mean Water Level flow conditions. The horizontal density gradients due to salinity variation have been neglected since vertical column is well mixed. In this study, the time step is considered to vary from 10 to 15 seconds, according to changes in the velocity and grid.

Model calibration for hydrodynamics

The model run started from 1400 h of 24.10.2008 to 0300 h of 03.11.2008 and tides and currents at observational locations were stored at 30 min interval and compared with the observations.

The model was calibrated with the observations by tuning the manning roughness coefficient. In this study the roughness coefficient used was 0.1. Results of tide comparison at station 3 and 5 are presented in the Figure 8. The modeled tide at station 3 is in agreement with the observed tide both in phase and amplitude. However, the model values deviated from observation in phase by 10 min at station 5 although they were in agreement in amplitude. The modeled currents were compared with the observations at 4 locations (Figure 9). The results show that the model values at station 1 are in agreement with observations with deviations of < 0.05 m/s. The deviation in high tide at station 3 is about 0.1 m/s. In the above two cases there is no significant phase shift. In the station 5 although the values are in agreement in amplitude, there is a phase lag of 10 min. The model comparison with the observations at station 4 indicates the deviations in both amplitude and phase. Since this location is in the creek and shallow (2 m below CD), the deviations are found. The model was also calibrated for the lagrangian path collected on 01.11.2008 (Figure 10). The observations show the path was elliptical. The model predicted trajectory closely followed the observed track. The total excursion lengths of the modeled and observed paths are 27 km. However, the deviation of path around 1.0 km is found in the low water slack. The observed path has more curvature than the predicted one resulting in the advancement of predicted path by nearly 30 min.

The model was run for obtaining the current vector field in spring flood and ebb. These are presented in Figures 11 and 12. The results indicate that maximum speeds of 1.2 m/s are modeled during flood and 1.3 m/s during ebb. The high current regime are found relatively offshore.

The crude oil spill of 500 t was considered for modeling. The model was run for two seasons, viz, monsoon and postmonsoon by introducing spill at 4 different locations (Stations 1, 2, 3 and 4). The wind speeds of 5 m/s and 7.5 m/s were considered for postmonsoon and monsoon conditions respectively. The wind directions considered were northeast in postmonsoon and southwest in monsoon season. Station 4 is the farthest location from the coast. A spill of crude during postmonsoon would move offshore according to the combined forcing of prevailing currents and winds as shown in Figure 13. However, during monsoon season, the spill would move towards the coastline (Figure 14). The time to reach the coast, length of the coastline affected, spread area and oil thickness are given in the following Table 1.

Table 1. Fate of the spilled oil during monsoon.

Season	Spill Location	Time to reach the coast (hour)	Amount of oil on intertidal region (m ³)	Spread area (m ²)	Coast length affected (m)	Oil Thickness (mm)
Monsoon	Station1	13	480	325	2800	0.101
	Station2	17	475	350	2100	0.107
	Station3	15	470	350	2600	0.067
	Station4	28	370	475	2800	0.05

Total evaporable component of the oil would be 20% of the spill quantity. The spill at station 1 which is nearest location would reach the coast between Dahanu and Golvad within 13 h from the spill occurs, while it takes 28 h to reach the Dahanu coast if it occurs at station 4 which is farthest from the coast. Oil to the tune of 480 m³ will be deposited on the intertidal segment in the event of spill at station 1. The spread area ranged from 0.5 to 1 km². The thickness varied from 0.05 to 0.1 mm.

Basing on the lengths predicted, areas of intertidal segment affected were calculated. Four different locations on the coast would be affected due to the spills. The intertidal distances at Golvad, Narpad, Dahanu and Gungvada are 3 km, 1 km, 1.5 km, 2.2 km and 2.1 km respectively. However all intertidal segment is generally not affected by the spill. In this work, it was considered that approximately 200 m stretch from neap low tide line to spring high tide line would be affected. Macrobenthos data was collected during July and November 2008 at Dahanu coast (Anonymous, 2010). This data is presented in Table 2.

Table 2. Observed macrobenthos biomass and populations

Segment	July 2008		November 2008	
	Biomass (gm/m ²)	Population /m ²	Biomass (gm/m ²)	Population /m ²
High Water	0.26	77	17.64	891
Low water	0.001	13	0.56	406
Average	0.26	45	9.1	649

The observations show that the macrobenthic biomass and population were more in the high tide line as compared to the low water level.

Using the coastline lengths and the observed benthos data, the total biomass and population affected were calculated. Average benthic biomass and population in the intertidal region are used in the calculations. It was considered that the oilspill would have covered upto 200 m from the low tide line. This data is presented in Table 3.

Table 3. Affected macrobenthos biomass and population due to oil spill.

Station	Biomass affected (Kg)	Population affected (/m ²)
1	145.6	2.5x10 ⁷
2	109.2	1.9x10 ⁷
3	135.2	2.3x10 ⁷
4	145.6	2.5x10 ⁷

The results indicate that relatively more damage is anticipated in case of spills occurred at station 1 and 4 as compared to the 2 and 3.

The major species affected would be polychaetes. This study will be extended and the model results will be compared with the observations of oil spill occurred due to ship collision on 07.08.2011 off Mumbai harbor.

Acknowledgements

We thank Dr. S. N. Gajbhiye, Scientist-in-Charge, Regional Centre, Mumbai and Dr. S. R. Shetye, Director, NIO for their keen interest in the work and for providing all necessary facilities. We are also grateful to Dr. R.S Kankara and Dr. B.R. Subramanian, ICMAM, Chennai who provided logistic support during field planning and observations. This work has been carried out under the oil spill modeling project, funded by Ministry of Earth Sciences, Government of India.

References

- Anonymous, 2010. Monitoring of Marine Ecology off Dahanu creek and adjacent coastal area due to release of FGD by REL-Thermal Power Station, June 2010, NIO/SP-37/2010, 44.
- Binliang Lin, Falconer, R.A., 1996. Numerical Modelling of three-dimensional suspended Sediment for estuarine and Coastal Waters. *Journal of Hydraulic Research*, 1996, 34, 435-454 pp.
- Blockker, P.C., 1964. Spreading and Evaporation of petroleum products on water, Proceedings , 4th International Harbor Congress, Antwerp, the Netherlands, 911-919.
- Brunet, M., Reddy, G. S., 1997. Modelling of Currents and Sediment Transport for the Prediction of Coastal Evolution, *Proceedings of the Fourth Int. Conf. Water Pollution 97, Modelling, Measuring and Prediction*, 1997, Bledslovenia.
- Clark, R.B., 1992. Marine Pollution, Third ed. Gookcraft Ltd., Great Britain, UK, 50-60.
- Cohen, Y., Mackay, D., Shiu, W.Y. J. 1980. Mass transfer rates between oil slick and water. *The Canadian Journal of Chemical engineering*, 58.
- Fay, J.A., 1969. The Spread of Oil slicks on a Calm sea, In Oil on the sea (ed. By D. Hoult), P. 53-64, Plenum, New York.
- Fay, J. A., 1971. Physical processes in the spread of oil on a water surface, Proceedings of the joint conference on prevention and control of oil spills, Washington, D. C., June, Amer. Petrol. Inst., 463-467 .
- Fay, J.A., 1971. Physical Processes in the Spread of Oil water surface, Proceedings of the oil conference on prevention control of oil spills, Washington, D.C., June, Amer Petrol Inst: 463-467.
- Fisher, H. B., List, E. J., Koh, R. CY., Imberger, J., Brooks, N. H., 1979. Mixing in Inland and Coastal Waters, Academic Press, New York.
- Gesteira J.L.G, Dauvin, J.-C., 2005. Impact of the Aegean Sea oil spill on the subtidal fine sand macrobenthic communityof the Ares-Betanzos Ria (Northwest Spain). *Marine Environmental Research* 60: 289–316.
- Huang, J.C., Monastero, F. C., 1982. Review of the state-of-the Art of oil spill simulation models, Amer. Petrol. Inst., Raytheon Ocean systems Company, East Providence, R. I. June.
- Kankara, R. S., Subramanian B. R., 2007. Oil spill sensitivity analysis and risk assessment for Gulf of Kachchh, India, using integrated modeling, *Journal Coastal Research* 23: 1251-1258 .
- Mackay, D. C.D. McAuliffe, 1980. Fate of Hydrocarbons discharged at sea, *Oil and Chemical Pollution* 5: 1-20.
- Mackay, D., Paterson, S., and Trudel, K., 1980. A mathematical model of oil spill behavior, Environmental Protection Service, Fisheries and environment Canada, Ottawa, Ontario,Canada.

- Reddy, G. S., Brunet Marc., 1997. Numerical Prediction of Oil-Slick movement in Gabes Estuary. International Conference on Coastal Engineering 97, La Coruna , Spain/23-25/ June, 1997.
- Reddy, G.S., Sharad Tripathi., 1998. “ Fluidyn-FLOWCOAST a software for prediction of Oil- Slick and Hydrocarbon transport in open water. “ International Conference on OIL SPILL 98, 29-31 July 1998, Southampton, UK.
- Reed, M, Spaulding, M. L, Gundlach, E. R, Kana, T.W, Siah, S. J, 1986. Formulation of a Shoreline/Oil Spill Interaction Model, Proceedings of the 9th Annual Arctic and Marine Oil Spill Program, 77-100.
- Shen, H.T., P.D. Yapa., 1988. Oil slick transport in rivers, *Journal of Hydraulic Engineering* 114. 529-543.
- Thomas A S., Andrews, H., Stevens, T., and David, R., 2011. Impacts of the Pacific Adventures Oilspill on the macrobenthos of subtropical sandy beaches, *Estuaries and coasts* 34: 937-949 .
- Thompson, J.F., Thames, F.C., Martin, C.W., 1977. TOMCAT- a code for numerical generation of body-fitted curvilinear coordinate system for filed containing any number of arbitrary two-dimensional bodies. *Journal of Computational Physics* 15: 299-319.
- Vethamony, P., Sudeesh, K., Babu, M.T., Jaya Kumar, S., Mani Murali, R., Saran A. K., Sharma L. H., Rajan B, Srivastava M., 2007. Trajectory of oil spill off Goa, Eastern Arabian Sea : Field observations and simulations., *Environmental Pollution* 148: 438-444 .
- Vethmony, P., Reddy, G. S., Babu, M. T., Desa, E., Sudeesh, K., 2005. Tidal eddies in semi-enclosed basin: A model study, *Marine Environmental Research* 59: 519-532.
- Yapa, P. D., Shen, H. T., Angamma, K., 1994. Modeling oil spill in a River-Lake system, *Journal of Marine Systems* 5: 453-471.
- Yapa, P. D., 1996. State-of-the-Art Review of Modeling transport and fate of oil spills, *Journal of Hydraulic Engineering*, 122, No 11.

List of Figures

Figure 1: Station Locations.

Figure 2: Tide at Station 3 and Station 5.

Figure 3: Current vectors at Station 1.

Figure 4: Current vectors at Station 3.

Figure 5: Current vectors at Station 5.

Figure 6: Current vectors at Station 4.

Figure 7: Model bathymetry.

Figure 8: Comparison of observed and predicted tide at Station 3 and Station 5.

Figure 9: Comparison of observed and predicted currents at Stations 3, 4 and 5.

Figure 10: Comparison of Lagrangian path collected on 01/11/2008.

Figure 11: Modeled current vectors during peak ebb.

Figure 12: Modeled current vectors during peak flood.

Figure 13: Oil spill trajectory during postmonsoon at (a) station 1, (b) station 2, (c) station 3 and (d) station 4.

Figure 14: Oil spill trajectory during monsoon at (a) station 1, (b) station 2, (c) station 3 and (d) station 4.

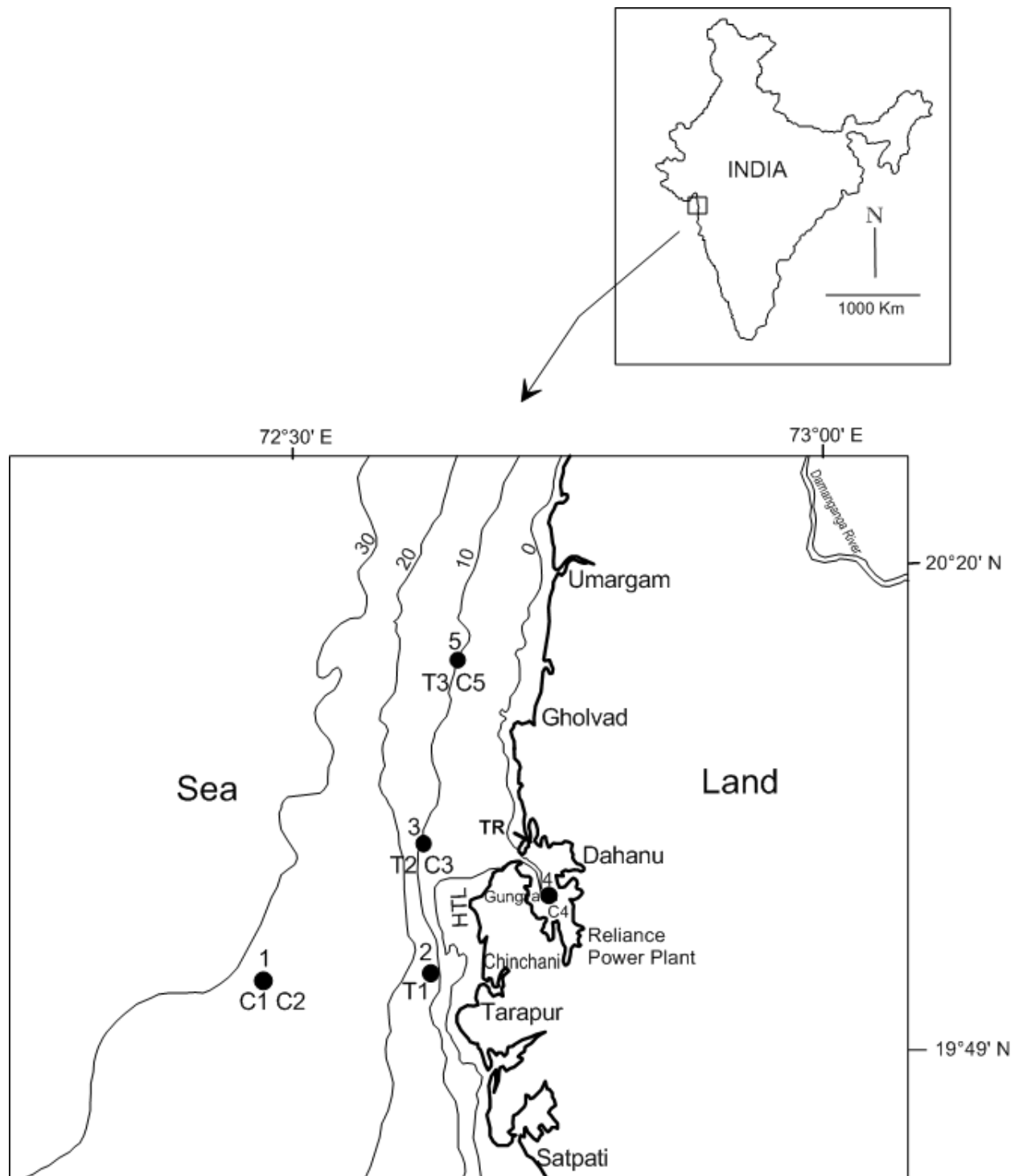


Figure 1

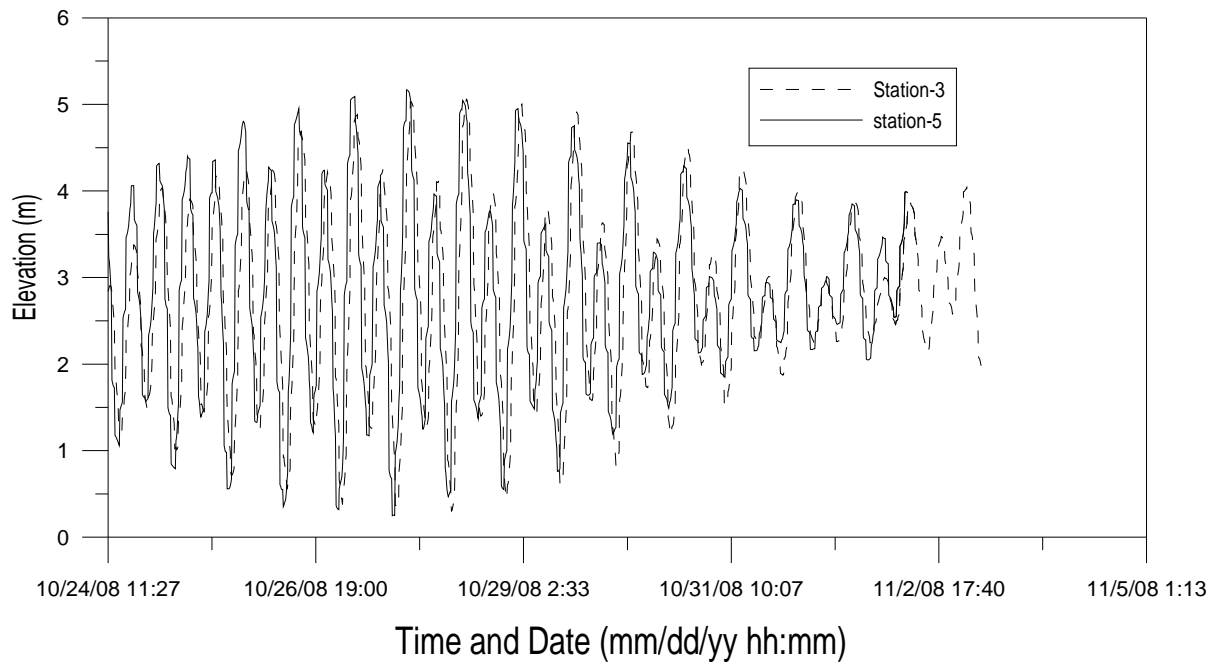


Figure 2

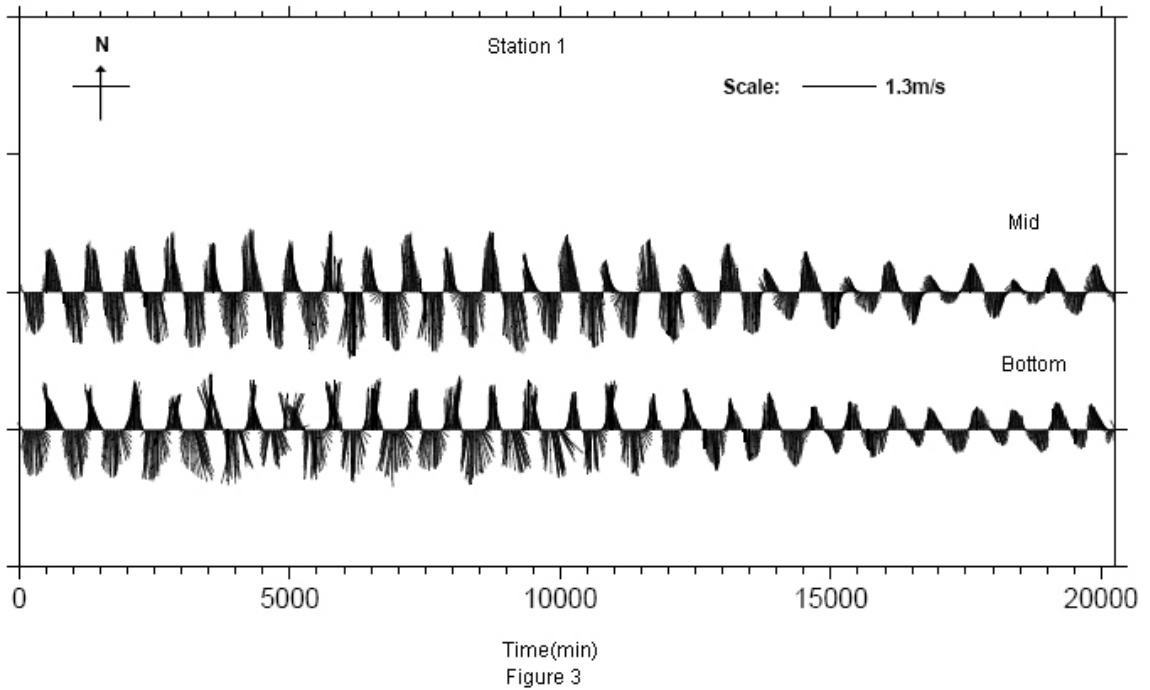
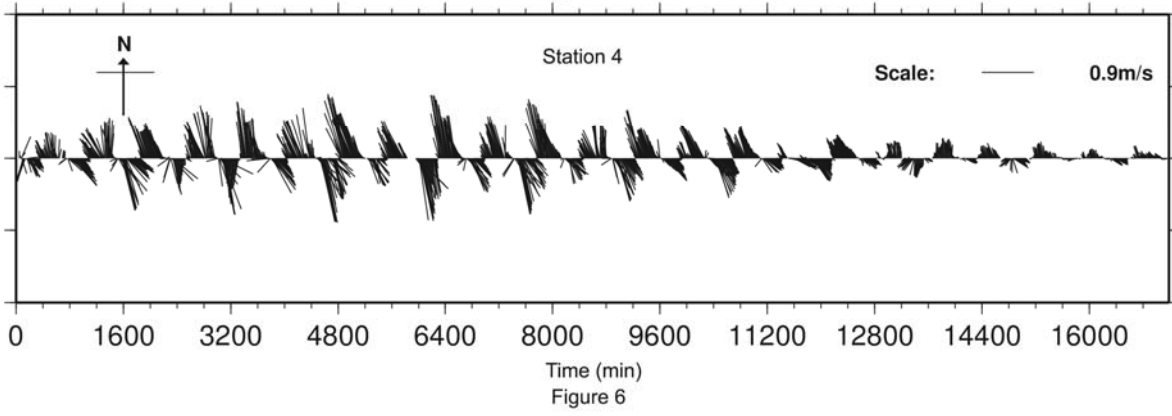
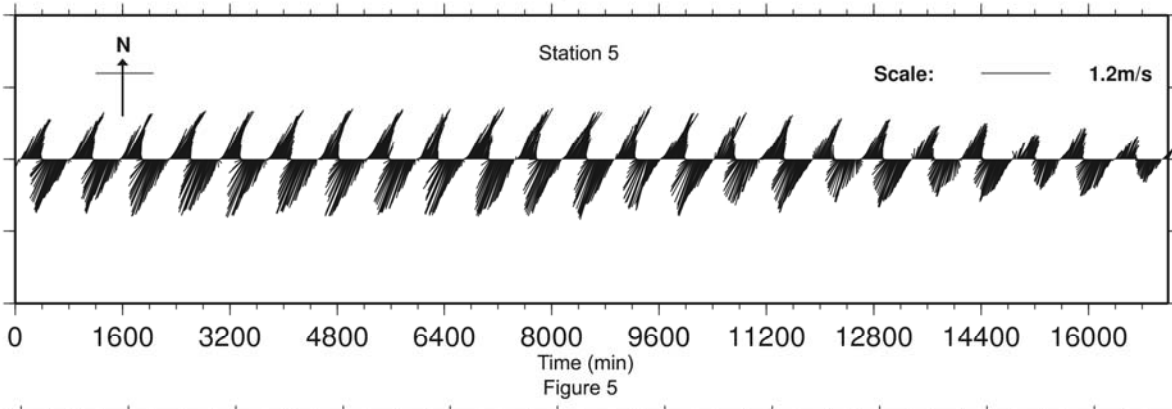
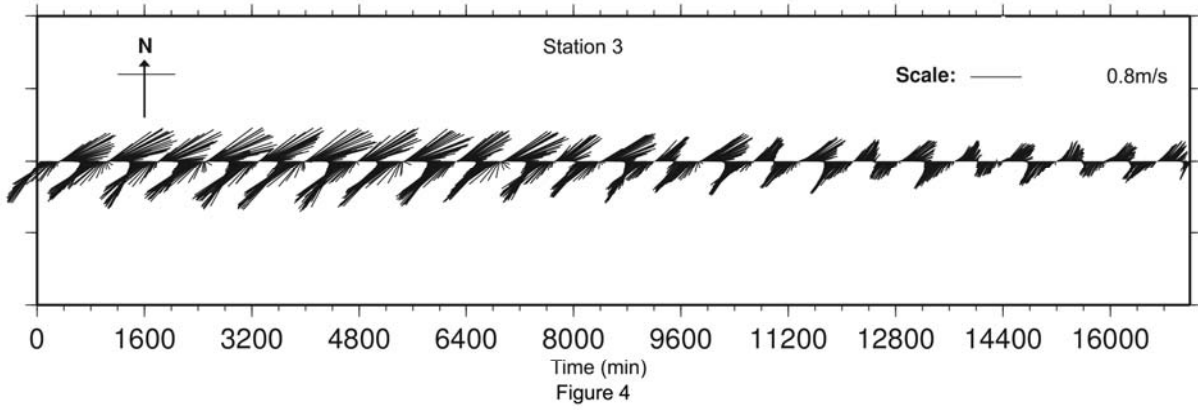


Figure 3



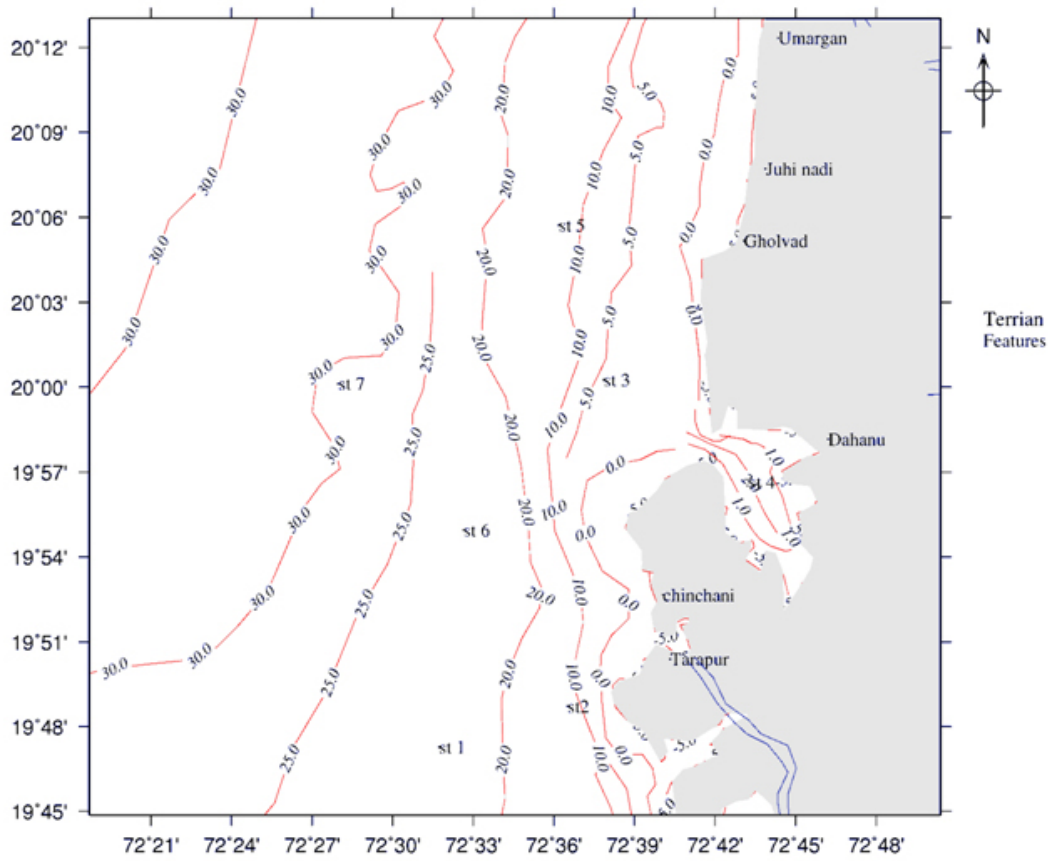


Figure 7

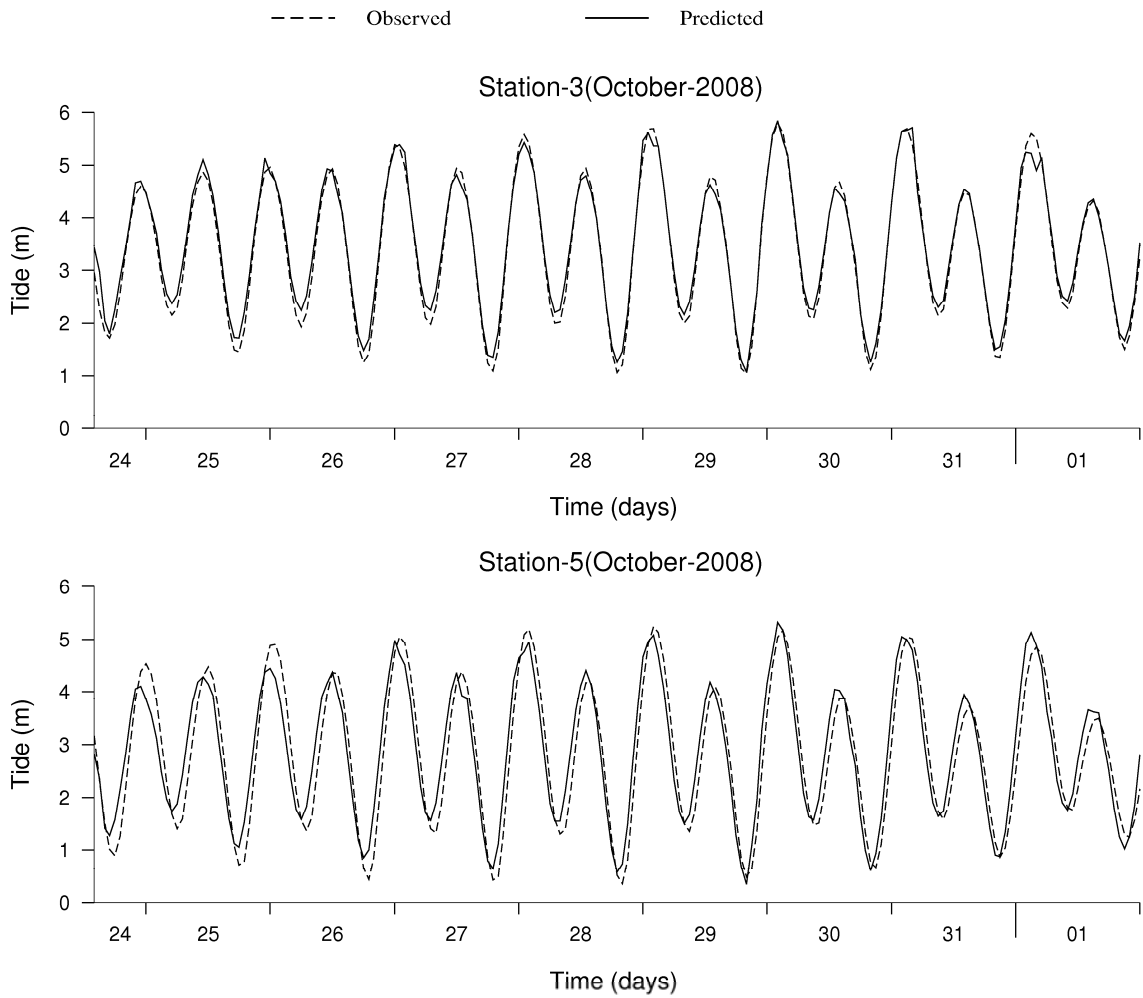


Figure 8

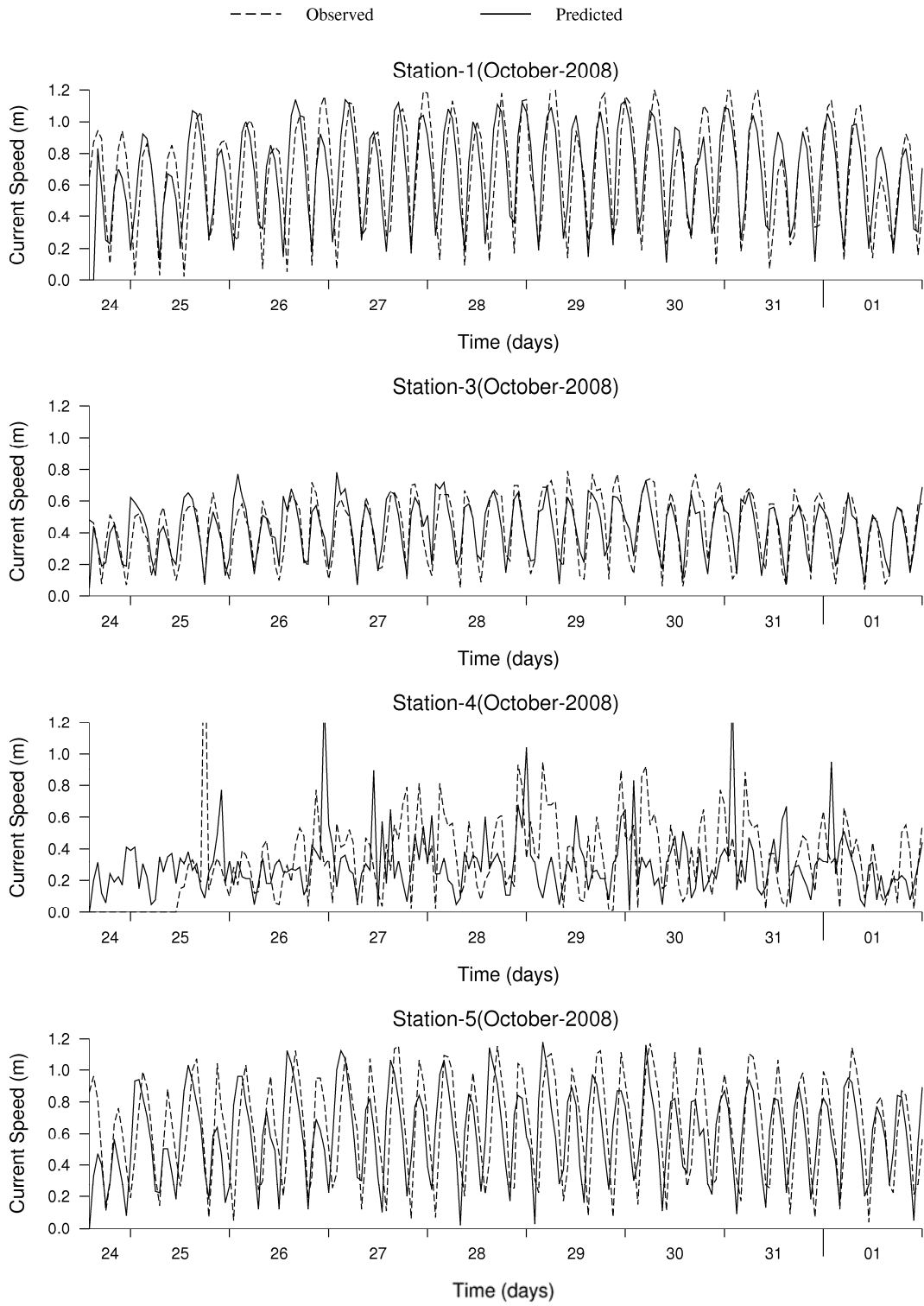


Figure 9

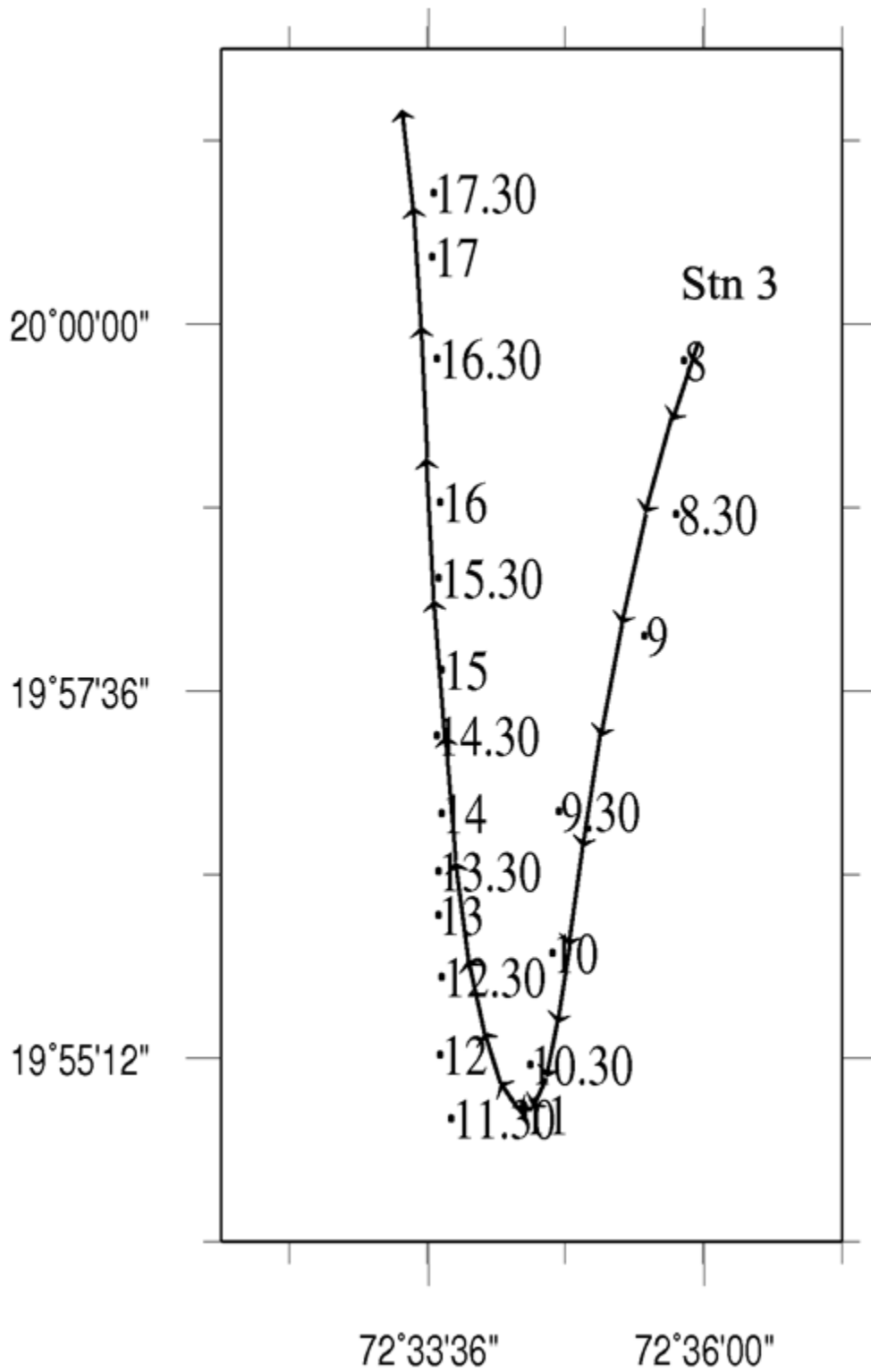


Figure 10

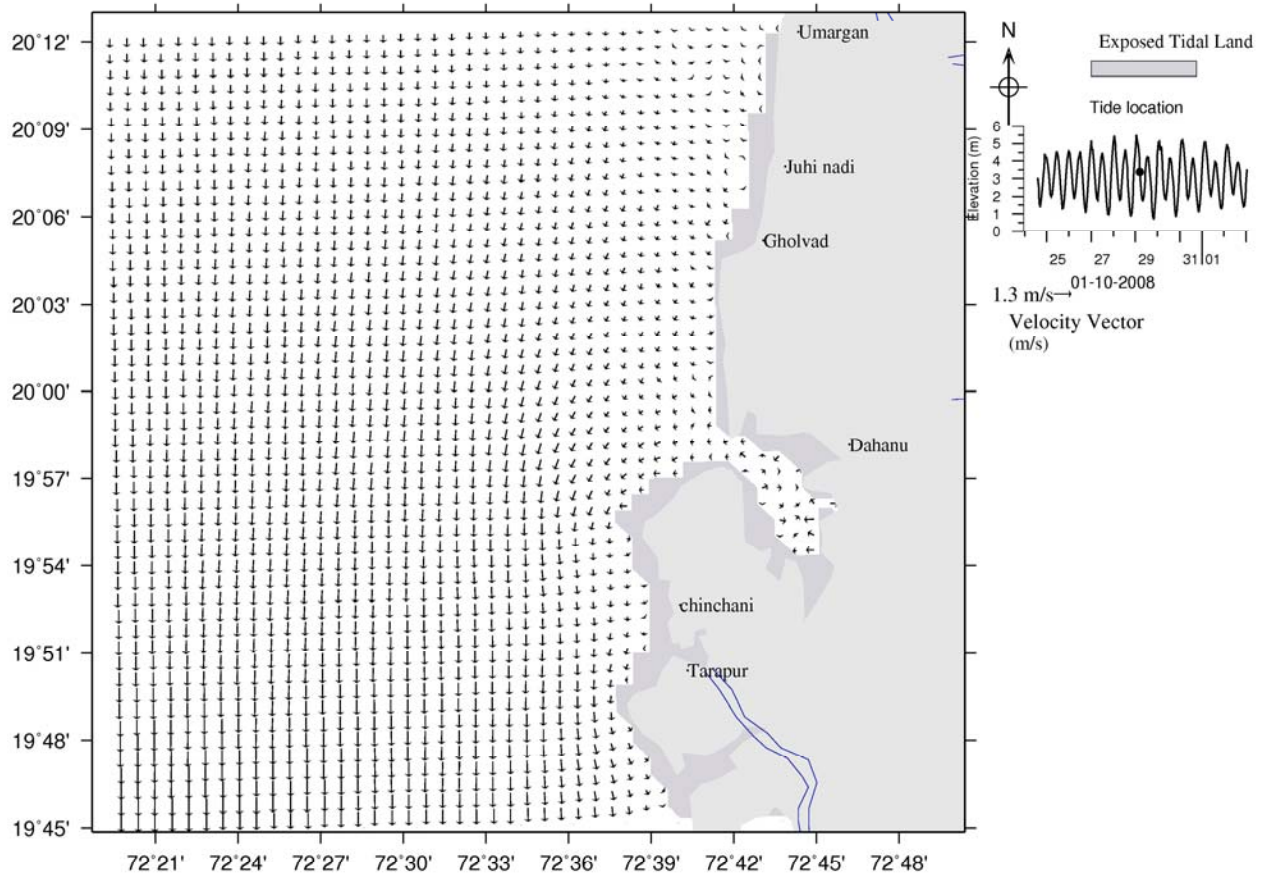


Figure 11

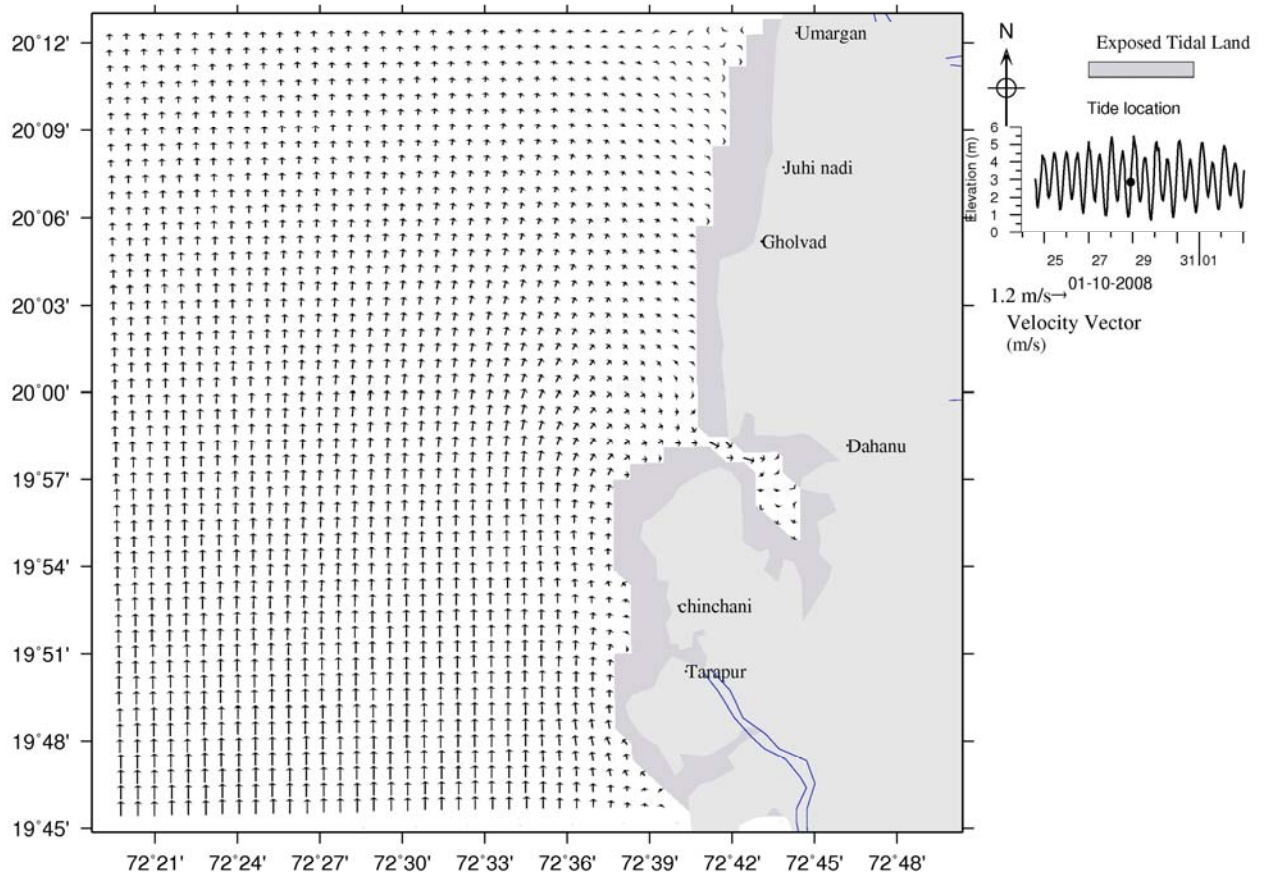


Figure 12

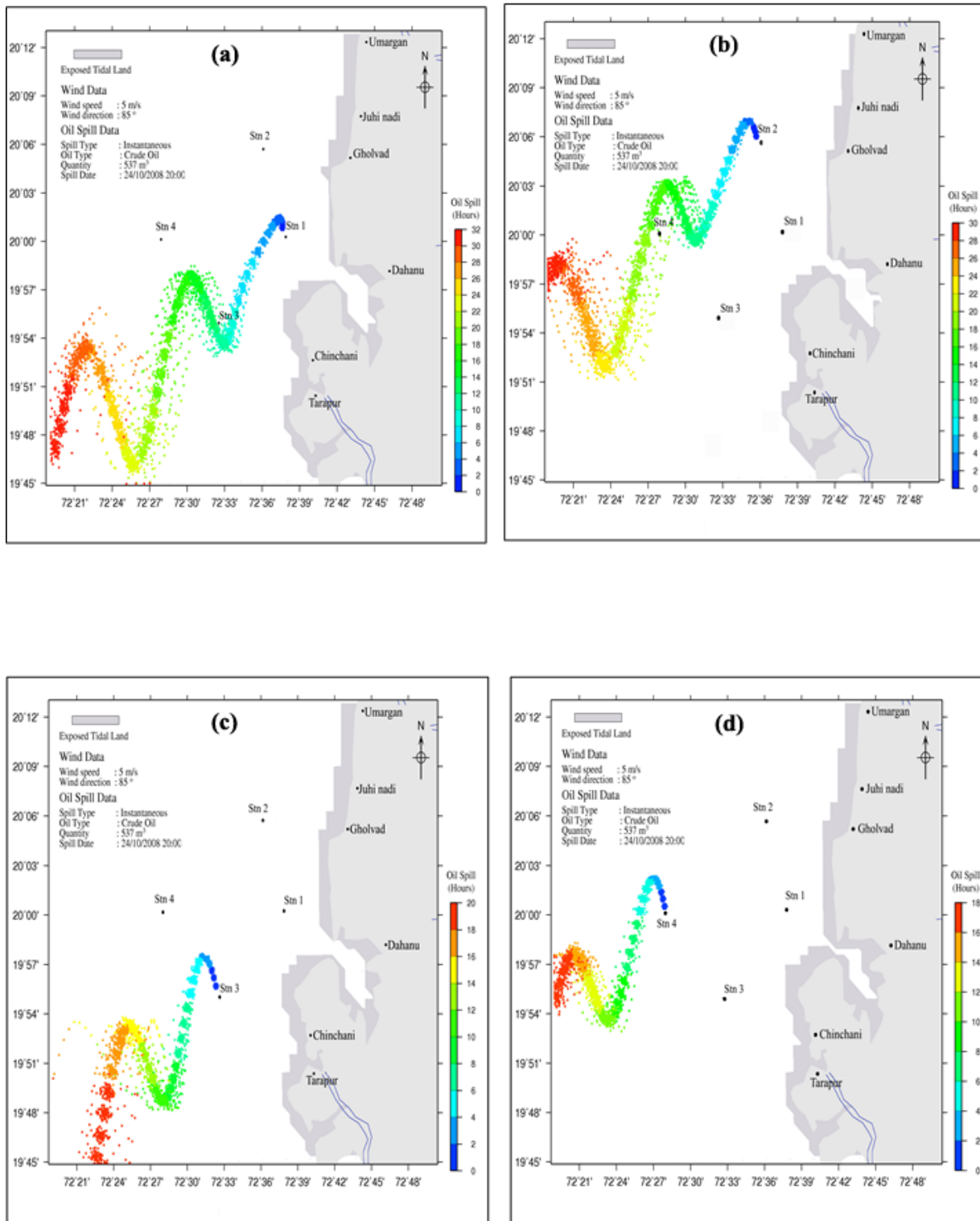


Figure 13

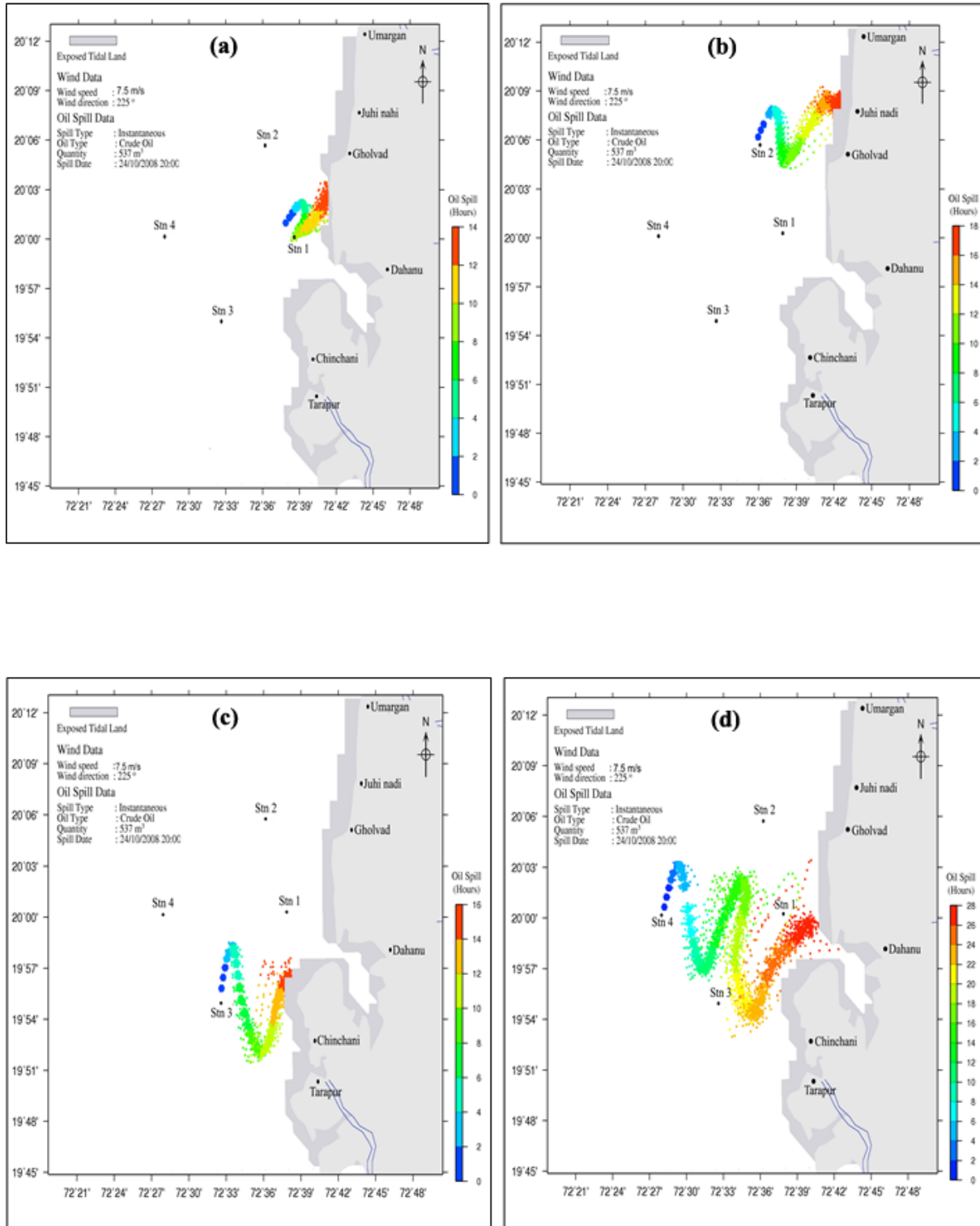


Figure 14